Angiopoietin-like 4 prevents metastasis through inhibition of vascular permeability and tumor cell motility and invasiveness.

Ariane Galaup, Aurélie Cazes, Sébastien Le Jan, Josette Philippe, Elisabeth Connault, Emmanuelle Le Coz, Halima Mekid, Lluis M. Mir, Paule Opolon, Pierre Corvol, et al.

Biological Sciences : Medical Sciences

ANGIOPOIETIN-LIKE 4 PREVENTS METASTASIS THROUGH INHIBITION OF VASCULAR PERMEABILITY AND TUMOR CELL MOTILITY AND INVASIVENESS

Ariane Galaup *†, Aurelie Cazes *†, Sebastien Le Jan *†, Josette Philippe *†, Elisabeth Connault ‡, Emmanuelle Le Coz *†, Halima Mekid *†, Lluis M. Mir ‡, Paule Opolon ‡, Pierre Corvol *†, Catherine Monnot *†, Stephane Germain *†§

* INSERM Unit 36, 11 place Marcelin Berthelot 75005 Paris - France,
† College de France, 11 place Marcelin Berthelot 75005 Paris – France,
‡ CNRS UMR 8121 IGR, 39 rue Camille Desmoulins, 94805 Villejuif – France,
§ Service d'Hematologie Biologique A – AP-HP - Hopital Europeen Georges Pompidou, Paris - France

Address correspondence to : Stephane Germain, INSERM U36 – College de France, 11 place Marcelin Berthelot 75005 Paris – France, Tel : 33 1 44 27 1664 ; Fax : 33 1 44 27 1691

E-Mail : stephane.germain@college-de-france.fr

Manuscript informations :

20 pages including Title, Abstract, Text, References and Figure legends

5 figures

Word and character counts :

Abstract : **218 words**

Abbreviations footnote :

ANGPTL4: Angiopoietin-like 4

TG: Triglycerides

VP: Vascular Permeability

ECM: Extracellular Matrix

ABSTRACT

Angiopoietin-like 4 (ANGPTL4), a secreted protein of the angiopoietin-like family is induced by hypoxia in both tumor and endothelial cells as well as in hypoxic perinecrotic areas of numerous cancers. Here, we investigated whether ANGPTL4 might affect tumor growth as well as metastasis. Metastatic 3LL cells were therefore xenografted into control mice and mice in which ANGPTL4 was expressed using *in vivo* DNA electrotransfer. Whereas primary tumors grew at a similar rate in both groups, 3LL cells metastasized less efficiently to the lungs of mice which expressed ANGPTL4. Fewer 3LL emboli were observed in primary tumors suggesting that intravasation of 3LL cells was inhibited by ANGPTL4. Furthermore, melanoma B16F0 cells injected into the retro-orbital sinus also metastasized less efficiently in mice expressing ANGPTL4. Although B16F0 cells were observed in lung vessels, they rarely invaded the parenchyma, suggesting that ANGPTL4 affects extravasation. In addition, recombinant B16F0 cells that overexpress ANGPTL4 were generated showing a lower capacity for *in vitro* migration, invasion and adhesion than control cells. Expression of ANGPTL4 induced reorganization of the actin cytoskeleton through inhibition of actin stress fibers formation and vinculin localization at focal contacts. Altogether, these results show that ANGPTL4 through its action on both vascular and tumor compartments prevents the metastastic process by inhibiting vascular activity as well as tumor cell motility and invasiveness.

INTRODUCTION

Understanding the molecular mechanisms that underlie tumor progression, local invasion and the formation of tumor metastases represents a major challenge in cancer research. Metastasis of tumor cells is the primary cause of death in patients with cancer (1). Cellular mechanisms controlling metastasis affect different tumor cell properties, such as cell locomotion or endothelial cell- and extracellular matrix (ECM) - tumor cell interation (2, 3). Numerous molecules, including growth factors and their receptors, have been reported to be involved in this process thereby supporting angiogenesis (4) and/or lymphangiogenesis (5). Among them, angiopoietins that bind to the Tie-2 receptors, have been shown to contribute to both angiogenesis and remodelling of lymphatic vessels. Angiopoietin-2-deficient mice form lymphatic vessels but have profound defects in lymphatic vessel remodeling, resulting in chylous ascites and defects in patterning and function of lymphatic vasculature (6), as well as impairment in the responsiveness of endothelial cells to pro-inflammatory cytokines (7). Also, angiopoietin-3 inhibits pulmonary metastasis by inhibiting tumor angiogenesis (8).

Recently, angiopoietin-like proteins, that do not bind to Tie-2 but contain motifs structurally conserved in angiopoietins have been identified. Among them, ANGPTL4, also known as hepatic fibrinogen/angiopoietin-related protein (HFARP) (9), and peroxisome proliferator-activated receptor-γ (PPARγ) angiopoietin-related gene (PGAR) (10) or fasting-induced adipose factor (FIAF) (11), is a circulating plasma protein, expressed in the liver, adipose tissue and placenta (10, 11). ANGPTL4 is up-regulated by fasting, by peroxisome proliferator-activated receptor agonists, associates with lipoproteins (12) and is involved in regulating glucose homeostasis, insulin sensitivity and lipid metabolism through its capacity to inhibit lipoprotein lipase (13, 14, 15).

Previous studies have shown that ANGPTL4 expression is regulated by hypoxia both in endothelial cells (16) and tumor cells (17). Moreover, *angptl4* mRNA is expressed in the perinecrotic areas of various human tumors and is highly upregulated in epithelial tumor cells from clear-cell renal carcinoma (16). Therefore, several studies have investigated the potential role of ANGPTL4 on angiogenesis. Kim *et al.* showed that ANGPTL4 protects endothelial cells from apoptosis through an endocrine action (9). We have reported an ANGPTL4-proangiogenic response in the chicken chorioallantoic membrane assay (16) whereas Ito *et al.* showed that ANGPTL4 inhibits VEGF-induced vascular leakiness and neoangiogenesis (18). Transgenic mice that express ANGPTL4 in the skin show impaired growth of subcutaneously

(s.c.) grafted CMT93 murine colorectal tumor cells associated with fewer intratumoral blood vessels (18). These findings suggest that ANGPTL4 exerts multiple biological functions in various contexts but its potential role in regulating metastases formation have not been investigated yet.

Here, we explored the effects of ANGPTL4 on intravasation, extravasation and growth of tumor cells in target organs during the metastatic process. We used plasmid DNA electrotransfer into skeletal muscle (19) to release ANGPTL4 into the systemic circulation in two established metastatic models (3LL s.c. injection and B16F0 i.v. injection). Using metastatic 3LL cells, we show that ANGPTL4 prevents metastasis through inhibition of tumor cell intravasation from the primary tumor to lymphatic or blood vessels without affecting angiogenesis or lymphangiogenesis. We also show that ANGPTL4 inhibits extravasation of B16F0 cells from the circulation to lungs, as well as vascular permeability. In addition *in vitro,* we used stably-transfected melanoma B16F0 cell lines expressing and secreting ANGPTL4, thereby demonstrating a direct autocrine effect of ANGPTL4 on B16F0 tumor cells through inhibition of migration, invasion, adhesion and cytoskeleton reorganization.

Together, these results show that ANGPTL4, through its action on both vascular and tumor compartments, is able to prevent the metastastic process through inhibition of vascular activity as well as tumor cell motility and invasiveness.

MATERIALS AND METHODS

Cell culture

Lewis lung carcinoma 3LL cells were cultured with RPMI medium supplemented with 10% fetal calf serum (FCS) and 1mM L-glutamine (Invitrogen). B16F0/ANGPTL4 cell lines were established by transfecting B16F0 cells with the full-length human *angptl4* cDNA in pcDNA3.1mycHis (Invitrogen) and by selecting three stably transfected clones (with -Low; -Medium or -High expression of ANGPTL4-mycHis) with geniticin (GIBCO BRL). A B16F0/Empty vector cell line was established by transfection with pcDNA3.1mycHis (Invitrogen) and was used as control for the *in vitro* study. Cells were maintained in MEM-Glutamax medium (Invitrogen) supplemented with 10% FCS.

Electrotransfer

Twenty micrograms of DNA resuspended in 20μl sterile saline were injected into each tibialis cranialis of 8-week old mice. Subsequently, one pulse of 800 V/cm and 100 μs of duration, followed one second later by a second pulse of 80 V/cm and 400 ms of duration (19), were delivered through two stainless steel parallel plates, 5mm apart, by a Cliniporator device (IGEA). Seven independent experiments were performed with two randomized groups (n=5 to 10 mice per group). The control group received pcDNA3.1-mycHis plasmid injections and the ANGPTL4 group was injected with pcDNA3.1-ANGPTL4-mycHis plasmid. Electrotransfer was performed two weeks before all *in vivo* experiments (3LL model n=3, B16F0 model n=2 and Miles assay n=2).

Metastatic models

Experiments were performed with 10-week old C57Bl/6 female mice. Cultured 3LL and B16F0 cells were resuspended in PBS at 1.10^7 cells/ml. Tumor 3LL cells (200μl) were injected subcutaneously (s.c.) into the flank of mice from ANGPTL4 and control groups. Sera, tumors, lymph nodes and lungs were weekly collected from control mice (n=5) and ANGPTL4 electrotransferred mice (n=5) during four weeks for expression and histology study. As for B16F0 cells, mice from ANGPTL4 and control groups received one intravenous (i.v.) injection of B16F0 cell suspension in volume of 50μl *via* the retro-orbital sinus. Lungs were collected, two or three weeks post-injection of tumor cells (p.i.).

Immunohistochemistry and image analysis

The different specimens (primary tumors, lymph nodes and lungs for the 3LL model and lungs for the B16F0 model) from all the mice studied in five experiments were fixed in Finefix (Milestone Medical), then paraffin sections (4μM thick), and hematoxylin-eosin-saffranin (HES) slides were prepared. For immunohistochemistry, tumor and lung sections were incubated with rat primary antibody raised against mouse CD34 (clone MEC 14.7, Hycult biotechnology). All the sections were analyzed using a Zeiss Axiophot microscope (Germany) and a Sensicam PCO digital camera (Germany). Representative views were taken at x100 magnification.

In the 3LL model, CD34- and HES-stained slides of the maximal sections of the primary tumors, of the lymph nodes and the lungs obtained from 40 mice (control or ANGPTL4 mice sacrificed at week 1, 2, 3 and 4) were analyzed by two independent operators. The emboli (tumor cells invading lumen of the vessels) were counted inside and at the vinicity of the primary tumors. The incidence, the volume of the metastatic lymph nodes, and the number of 3LL micrometastases in lungs, were also determined.

CD34- and HES-stained slides of the lungs obtained from the 12 mice i.v. injected with B16F0 and sacrificed 2 week p.i. were observed by two independent operators to distinguish and count micrometastases that had implanted into the lung parenchyma from emboli that had remained intravascular.

The lungs of 13 mice i.v. injected with B16F0 and removed three week p.i. were analyzed for the assessment of the development of macrometastases. HES-stained sections of these lungs were digitized with a slide scanner (Nikon SuperCoolscan 8000 ED; Nikon). As previously published, a dedicated script was implemented to the PIXCYT software (20) in order to determine the total metastatic surface per mouse and the mean surface per metastasis. Analysis of 57 metastases for the control group and 21 metastases for the ANGPTL4 group was performed by two different operators.

Miles assay

Female 10-week-old athymic *nude* mice from ANGPTL4 and control groups were anesthetized and 200μl of 1% Evans blue dye (Sigma) were injected into tail vein. Five min after the dye injection, 20μl of histamine (1 and 10 nM) or PBS were intradermally injected in the side of the mouse back. Skin surrounding the injected sites was removed 20min later, weighed and the blue dye was extracted from skin with formamide during 48h at 37°C. The amount of extravasated dye was measured with a spectrophotometer (610 nm). For each

group, leakiness was reported in ng of Evans blue per milligram of fresh tissue. Values shown are the mean ± SEM (n= 3 mice per condition).

Western blotting

To detect the presence of ANGPTL4 in mice sera after *in vivo* electrotransfer, blood samples were collected two and six weeks after electrotransfer from ANGPTL4 and control mice. As control and semi-quantitative method, 1µg of recombinant ANGPTL4-mycHis protein was injected into tail vein of 10-week old C57Bl/6 female mice and 30min later blood samples were collected. For *in vitro* analysis, B16F0/Empty vector and B16F0/ANGPTL4-Low, -Medium or -High cells were plated into T75-flask in serum free medium. Culture supernatants were collected after 48h and concentrated with Amicon Ultra filters (Millipore). Culture supernatant of CHO cells expressing ANGPTL4 (16) was included as control. Western blots were probed with antibody directed against c-myc tag (clone 9E10, Roche) and detected with a biotin-streptavidin system.

Enzymatic determination of triglycerides in mice blood

Recombinant ANGPTL4-mycHis protein was purified from stably transfected CHO cells by affinity chromatography (Cobalt affinity column Talon, BD Biosciences). Then, 200μl containing either 0, 1, 10 or 50µg purified ANGPTL4 were injected into tail vein of 10-week old C57Bl/6 female mice (n=12). Blood samples were collected 30min after injection, and plasma triglycerides (TG) were measured by enzymatic reaction (TG PAP 150 kit, Biomerieux). Values shown are the mean ± SEM (n= 3 mice per condition).

Adhesion assay

Culture plates (24-well) were coated with BSA, fibronectin, laminin or vitronectin (10µg/ml) for 30min at 37°C, washed and blocked with 1% PBS/BSA for 30min at 37°C. B16F0/Empty vector and B16F0/ANGPTL4-Low, -Medium or -High cells were prestained with calcein AM (5µg/ml, Molecular Probes) for 30min at 37°C. Stained cells (5.10^5) were plated and allowed to adhere for 1h at 37°C. Non adherent cells were washed away three times with PBS and the fluorescence of the cells was measured using a computer-based fluorescence reader (Fusion™, Packard Bioscience Company). All conditions were performed in triplicate. Values shown are the mean ± SEM of three independent experiments.

Migration and invasion assays in Boyden chambers

Migration and invasion assays were performed using HTS Fluoroblok 24-well chambers containing filters with 8µm pore size (BD Biosciences). For the migration assay, filters were precoated on the lower side with fibronectin (10μg/ml). For the invasion assay, filters were precoated on the upper side with Matrigel (20μg/well, BD Biosciences). Serum-free conditioned medium from NIH3T3 cells cultured for 18h was placed on the lower compartment of the chamber. B16F0/Empty vector and B16F0/ANGPTL4-Low, -Medium or -High cells were prestained with calcein AM (5µg/ml, Molecular Probes) for 30min at 37°C and 10^5 cells were seeded in serum-free MEM on the upper compartment of the chambers for 6h at 37°C. The fluorescence of the cells in the lower side of the filter was measured in the wells using a computer-based fluorescence reader (Fusion™, Packard Bioscience Company). All conditions were performed three times in triplicate. Values shown are the mean $\pm$ SEM.

Immunofluorescence assays

Glass coverslips coated with fibronectin (10µg/ml) or BSA (10µg/ml) for 1h at 37°C, then washed and blocked with 1% PBS/BSA for 30min. Control and ANGPTL4 cells were added and cultured for 48h in complete medium. Actin was visualized with rhodamine-phalloidin (Molecular probes) and vinculin was detected with clone H20.1 (Sigma). The cytoskeleton reorganization was evaluated as percentage of spread cells with actin stress-fibers and vinculin focal adhesions following adhesion of control and ANGPTL4 cells . For each condition (fibronectin or BSA), more than 100 cells were considered by two different evaluators and the experiments were independently performed three times. Values shown are the mean $\pm$ SEM.

Statistical analysis

Statistical analysis was performed and p values were calculated according to Student's t-test. Significant differences were accepted for $p<0.05$.

RESULTS

In vivo angptl4 gene transfer by electrotransfer

We first studied whether pcDNA3.1-ANGPTL4-mycHis plasmid injection in *Tibialis cranialis* combined with electrotransfer, allowed a stable and a long term production of secreted ANGPTL4 protein. As shown in Fig. 1 *A*, ANGPTL4 was detected by western-blot two and six weeks after electrotransfer (lane 2 and 3), in sera from mice injected with pcDNA3.1-ANGPTL4-mycHis plasmid as compared to control mice injected with pcDNA3.1-mycHis empty plasmid (lane 1). Moreover, as shown comparing lanes 2 (two weeks after ANGPTL4 electrotranfer) and 4 (injection of 1µg of the recombinant ANGPTL4), electrotransfer allowed the production of low levels of ANGPTL4 (below 1µg). In order to determine whether this tagged version of ANGPTL4 was active *in vivo*, we also determinated the level of TG in plasma of mice injected with various doses of recombinant ANGPTL4. Systemic injection of 50μg purified recombinant ANGPTL4 significantly increases plasma TG as compared to the injection of elution buffer (156$\pm$3 *versus* 71$\pm$5mg/dl, p=0.007). Lower levels of circulating protein (10 and 1μg) as well as the amount of electrotransferred protein used in this study did not significantly modify plasma TG (Fig. 1 *B*). Then, in order to avoid any confounding role of ANGPTL4 on TG we here study the effect of sustained but low levels of ANGPTL4 obtained after electrotransfer (<1μg), on tumor growth and metastasis.

ANGPTL4 inhibits 3LL tumor cells intravasation, invasion of lymph nodes and lung metastases

Murine 3LL cells, which mimic metastasis from primary tumor to lung were s.c. injected in mice in order to evaluate whether circulating ANGPTL4 might affect tumor growth as well as the metastatic process. Four weeks after 3LL cell injection, no significant difference in primary tumor volumes or in the number of intratumoral blood and lymphatic vessels were observed in ANGPTL4 expressing mice compared to control mice (data not shown). In contrast, as shown in Fig. 2 *A*, the incidence of emboli, defined as the presence of tumor cells within vessels inside tumors or at its vinicity (see arrows) was decreased in ANGPTL4 mice (see arrow, 14.6$\pm$1.4% *versus* 56.3$\pm$4.5%, p=0.04). This phenomenon correlated to the inhibition of local invasion to lymph nodes (Fig.2 *B*) and distant metastases formation to lungs (Fig. 2 *C*) observed in ANGPTL4 mice. Indeed, a decreased number of invaded lymph nodes was observed in ANGPTL4 mice compared to control mice all along the course of the

study (0/5 invaded lymph node *versus* 4/5 at week 2, and 3/5 invaded lymph nodes *versus* 5/5 at week 4) (Fig.2 *B*, left panel). In addition, mean volume of metastatic lymph nodes was also diminished in ANGPTL4 mice compared to control (19.8±9.8 *versus* 42.0±5.0mm^3 at week 3 and 76.8±8.4 *versus* 110.4±17.2mm^3 at week 4, $p<0.05$) (Fig.2 *B*, left and right panel).

As for distant invasion, incidence of lung metastases formation was lower in ANGPTL4 *versus* control group from week 1 (0/5 *versus* 3/5 mice) to week 4 (1/5 *versus* 5/5 mice). Mean number of metastases was also diminished (4.0±1.3 *versus* 0.2±0.2 in ANGPTL4 mice, $p=0.016$, Fig. 2 *C,* left and right panel). These data therefore suggest that ANGPTL4 inhibits intravasation of metastatic 3LL cells from the primary tumor leading to fewer local and distant metastases.

ANGPTL4 inhibits extravasation macrometastases formation.

In order to evaluate any role of ANGPTL4 on the extravasation step of tumor cells, we also used B16F0 melanoma cells which when i.v. injected, survive, extravasate, divide and form lung metastases. B16F0 cells were i.v. injected into ANGPTL4 electrotransferred or control mice which were then sacrificed 2 weeks p.i.. Then, lungs were examined for tumor islets and tumor cells that have invaded into the lung parenchyma (micrometastases) were distinguished from tumor cells that remained within intact vessel lumens (emboli) using HES and CD34-staining (Fig. 3 *A*). In the control group, many micrometastases were established (13.5±4.2) and no intravascular tumor cells i.e. emboli remained. As contrast, 1.5±1.2 micrometastases and 1.5±1.4 emboli were observed in the ANGPTL4 group ($p=0.023$, Fig. 3 *B* and 3 *C*), suggesting that ANGPTL4 inhibits B16F0 tumor cells extravasation.

In order to appreciate the development of large metastases, B16F0 cells were i.v. injected in ANGPTL4 or control mice, and mice were sacrificed after three weeks. Macroscopically, examination of lungs showed a reduced number of macrometastases in ANGPTL4-expressing mice (Fig. 3 *D-top panel*). Quantification from HES-stained lung sections (Fig. 3 *D-bottom panel*) showed that the total tumor surface in ANGPTL4 mice was decreased (3.9±0.9mm^2) compared to control mice (12.0 ± 0.8mm^2, $p=0.004$) (Fig. 3 *E*). As shown in Fig. 3 *F*, quantification of the mean tumor surface per macrometastasis revealed no significant difference between both groups (0.8±0.2mm^2 *versus* 0.7±0.1mm^2, $p=0.455$). These data suggest that whereas ANGPTL4 inhibits metastases seeding it does not affect proliferation when implanted into the target organ.

Inhibition of histamine-induced vascular permeability by ANGPTL4

As metastasis depends on tumor-endothelial cell interaction and vascular permeability (VP), we investigated whether ANGPTL4 inhibition of intravasation and extravasation might be, at least in part, explained by decrease in VP, as previously shown in transgenic mice (18). Miles assays performed in response to injection of 1 or 10nM histamine were used to induce VP in ANGPTL4 and control mice. As shown in Fig. 4, vascular permeability induced by 10nM histamine was significantly lower in ANGPTL4 mice compared to control mice (56.3±2.7 *versus* 91.8±0.9ng Evans blue/mg of fresh tissue, p=0.002).

ANGPTL4 inhibits tumor cell motility and invasiveness

To determine whether ANGPTL4 might directly modify tumor cell behavior, we stably transfected B16F0 cells either with an ANGPTL4 expressing plasmid (ANGPTL4 cells) or an empty vector (control cells). As shown in Fig. 5*A* and in accordance with previous reports (21), ANGPTL4 was produced as both full-length (50 kDa) and truncated-form (35 kDa) into cultured medium. Three clones showing three different levels of expression, (-Low, -Medium or -High), were used for *in vitro* characterization. No significant difference was observed in proliferation, cell viability, cell cycle or apoptosis between control cells and ANGPTL4 cells (data not shown). However, whatever the expression level, adhesion to various supports such as BSA, fibronectin, laminin or vitronectin was significantly inhibited in cells expressing ANGPTL4 compared to control cells (inhibition from 17.0 to 35.0% for B16F0/ANGPTL4-High, Fig. 5 *B*).

The effect of ANGPTL4 expression on tumor cell motility was then evaluated using a Boyden chamber assay. As shown in Fig.5 *C,* migration of ANGPTL4 cells was significantly reduced compared to control cells (inhibition of 28.5±0.6% for B16F0/ANGPTL4-High, $p=4.10^{-5}$). Furthermore, invasion through Matrigel was decreased in ANGPTL4 cells compared to the control cells (inhibition of 25.4±1.4% for B16F0/ANGPTL4-High, $p=9.10^{-5}$, Fig. 5 *D*). Together, these experiments indicate that ANGPTL4 inhibits tumor cell motility, adhesion and invasiveness.

ANGPTL4 modifies cytoskeleton organization

The inhibitory effect of ANGPTL4 in cell motility might suggest that ANGPTL4 affects cell spreading and cytoskeleton organization. As shown in Fig. 5*E*, B16F0 control cells display a classical well-organized cytoskeleton with many polymerized actin stress fibers (red staining) and attached cells *via* vinculin focal adhesions (green staining). In comparison, the

cytoskeleton of ANGPTL4 cells lacked stress fibers and showed a diffused vinculin-localization pattern. Quantification of cells showing a well-organized cytoskeleton on BSA or fibronectin confirmed that ANGPTL4 inhibits cell spreading and cytoskeleton organization even in low expressing cells (Fig. 5*F*). On fibronectin, well-organized cytoskeletons were observed in 72.1±9.2% B16F0 control cells *vs* 52.4±6.4% of B16F0/ANGPTL4-Low cells ($p=0.001$), 47.1±7.5% of B16F0/ANGPTL4-Medium cells ($p=4.10^{-4}$), and 36.1±3.1% of B16F0/ANGPTL4-High cells ($p=4.10^{-7}$).

DISCUSSION

In the present study, we provide evidence that ANGPTL4 inhibits metastasis, and we identify the steps on which ANGPTL4 may exert its action (intravasation, extravasation or metastasis development into target organ), as well as the cell types (tumor or vascular) and the mechanisms that are affected by ANGPTL4. Using DNA electrotransfer, we were able to produce low (below 1μg) and sustained levels of circulating ANGPTL4 in mice. This method was chosen in order to avoid any confounding role of ANGPTL4 on metabolism since as previously published by others (12, 13, 22), we show that only higher levels (above 50 μg) of ANGPTL4 protein are able to acutely induce increase of TG in the plasma.

First, we showed that ANGPTL4 inhibits metastasis by modulating intravasation of tumor cells. This phenomenon represents the first step of the metastatic process and implies the presence of blood vessels and lymphatics within and around the tumor as well as interactions between tumor and endothelial cells. Unlike angiopoietins and other members of the angiopoietin-like family that have been shown to regulate angiogenesis, namely ANGPTL1 (23, 24), ANGPTL2 (24) and ANGPTL3 (25), ANGPTL4 did not affect lymph or blood vessels density of primary Lewis lung carcinoma (3LL) tumors but decreased their *in vivo* intravasating potential.

Then, following entry into the circulation and before formation of metastases into target organs, tumor cell extravasation is required. Tumor cells are arrested through an intimate interaction with endothelial cells, followed by basement membrane degradation. We show here that ANGPTL4 inhibits the extravasation step. Indeed, the number of B16F0 micrometastases within the lung parenchyma is markedly decreased in mice that express ANGPTL4 compared to control mice. Instead of implanted metastases, emboli mostly remained intravascular in the ANGPTL4-electrotransferred mice. In addition, micrometastases which developed as macroscopic tumors were also fewer in ANGPTL4 mice, but their size was not significantly different, suggesting that, whereas B16F0/ANGPTL4 cells deposits were more rarely observed in the lung, their growth into the target organ was not affected. Interestingly, the overall survival of mice was not affected (data not shown), suggesting that the mice died from either development of the primary tumor itself, which was not affected by ANGPTL4 expression, or that despite the fact that fewer metastases were able to develop, these were sufficient to induce mice death.

The mechanisms of the anti-metastatic effect of ANGPTL4 were further investigated. First, alterations of vascular properties were shown to be induced by ANGPTL4. Indeed, we

showed that ANGPTL4 inhibits histamine-induced permeability, in accordance with a previous study that reported inhibition of VEGF-induced vessel leakiness by ANGPTL4 (18). This property has also been observed with angiopoietin 1 (26). These data suggest that endothelial cells may be a target of ANGPTL4, an observation which is consistent with previous studies (9, 18) and our unpublished observations.

In addition, we showed that ANGPTL4 also acts on tumor cells. Using recombinant murine melanoma B16F0/ANGPTL4 cells stably secreting ANGPTL4 at various levels, we showed inhibition of tumor cell migration, invasion and adhesion compared to B16F0 control cells. We further showed that ANGPTL4 affects cytoskeleton organization and focal adhesions formation. Disruption of actin stress fibers and focal adhesions, structures that link the cytoskeleton to integrins and the ECM (27) induces decreased adhesion, traction, and consecutively directional invasion and migration. The inhibition of cytoskeleton organization was more potent in highly expressing cells compared to medium or low expressing cells whereas inhibition of both migration, invasion and adhesion was comparable in these three cell lines suggesting that low levels of ANGPTL4 are sufficient to confer the observed inhibition *in vitro*.

The intravasation and extravasation steps during the metastasis process are regulated by a variety of molecules including: cell-cell and cell-ECM receptors, proteolytic enzymes involved in the breakdown of the basal membrane and invasion of vascular channels and organs, motility factors allowing migration through tissues, receptors mediating organ specific invasion. E-cadherin and its associated catenin complex (28) as well as Connexin 26, through heterologous gap junction formation with endothelial cells (29) play a crucial role in intravasation and extravasation of tumor cells. The potential modulation of homotypic and heterotypic cell interactions by ANGPTL4 therefore requires further investigations. Finally, integrins are a class of ECM receptors which trigger specific intracellular pathways to initiate distinct cellular responses, such as actin cytoskeleton assembly or cell adhesion and migration, properties that are modulated by ANGPTL4 in the present study. Among the integrins, β1 integrin is crucial for adhesion, spreading and motility of tumor cells (30) and plays a critical role in CXCR4-mediated B16 tumor cell metastasis (31). Whether ANGPTL4 effect on tumor cells is mediated through integrin activity is presently under study. Altogether, these results suggest that ANGPTL4, synthesized in response to hypoxia participates in the conditionning of the tumor microenvironment thereby affecting vascular activity as well as tumor cell motility and invasiveness leading to inhibition of metastases.

AKNOWLEDGEMENTS

We thank SCEA for animal care. AG is supported by a grant from la Fondation Lefoulon Delalande/Institut de France. SG belongs to the European Vascular Genomics Network supported by the European Community's sixth Framework Programme for Research Priority (Contract N° LSHM-CT-2003-503254). SG is supported by grants from la Fondation de France and Canceropole-PACA ACI 2004. This work was supported in part by a grant from Novartis. We thank Eric Etienne for the help provided for confocal microscopy and Steven Suchting for critical reading of the manuscript.

REFERENCES

1. Fidler, IJ.Critical determinants of cancer metastasis: rationale for therapy. (1999) *Cancer Chemother Pharmacol.* **43**, S3-10.

2. Crissman, J. D., Hatfield, J. S., Menter, D. G., Sloane, B., Honn, K. V. Morphological study of the interaction of intravascular tumor cells with endothelial cells and subendothelial matrix. (1988) *Cancer Res.* **14**, 4065-4072.

3. Hynes, R. O. Integrins: bidirectional, allosteric signaling machines. (2002) *Cell.* **6**, 673-687.

4. Carmeliet, P. Angiogenesis in health and disease. (2003) *Nat Med.* **6**, 653-660.

5. Achen, M. G., McColl, B. K., Stacker, S. A. Focus on lymphangiogenesis in tumor metastasis. (2005) *Cancer Cell.* **2**, 121-127.

6. Gale, N.W., Thurston, G., Hackett, S.F., Renard, R., Wang, Q., McClain, J., Martin, C., Witte, C., Witte, M. H., Jackson, D., *et al.* Angiopoietin-2 is required for postnatal angiogenesis and lymphatic patterning, and only the latter role is rescued by Angiopoietin-1. (2002) *Dev Cell.* **3**, 411-423.

7. Fiedler, U., Reiss, Y., Scharpfenecker, M., Grunow, V., Koidl, S., Thurston, G., Gale, N.W., Witzenrath, M., Rosseau, S., Suttorp, N., *et al.* Angiopoietin-2 sensitizes endothelial cells to TNF-alpha and has a crucial role in the induction of inflammation. (2006) *Nat Med.* **12**, 235-9.

8. Xu, Y., Liu, Y. J., Yu, Q. Angiopoietin-3 inhibits pulmonary metastasis by inhibiting tumor angiogenesis. (2004) *Cancer Res.* **17**, 6119-6126.

9. Kim, I., Kim, H. G., Kim, H., Kim, H. H., Park, S. K., Uhm, C. S., Lee, Z. H., Koh, G. Y. Hepatic expression, synthesis and secretion of a novel fibrinogen/angiopoietin-related protein that prevents endothelial-cell apoptosis. (2000) *Biochem J.* **346**, 603-610.

10. Yoon, J. C., Chickering, T. W., Rosen, E. D., Dussault, B., Qin, Y., Soukas, A., Friedman, J. M., Holmes, W. E., Spiegelman, B. M. Peroxisome proliferator-activated receptor gamma target gene encoding a novel angiopoietin-related protein associated with adipose differentiation. (2000) *Mol Cell Biol.* **14**, 5343-5349.

11. Kersten, S., Mandard, S., Tan, N. S., Escher, P., Metzger, D., Chambon, P., Gonzalez, F. J., Desvergne, B., Wahli, W. Characterization of the fasting-induced adipose factor FIAF, a novel peroxisome proliferator-activated receptor target gene. (2000) *J Biol Chem.* **37**, 28488-28493.

12. Mandard, S., Zandbergen, F., van Straten, E., Wahli, W., Kuipers, F., Muller, M, Kersten, S.

The fasting-induced adipose factor/angiopoietin-like protein 4 is physically associated with lipoproteins and governs plasma lipid levels and adiposity. (2006) *J Biol Chem.* **281**:934-44.

13. Yoshida, K., Shimizugawa, T., Ono, M., Furukawa, H. Angiopoietin-like protein 4 is a potent hyperlipidemia-inducing factor in mice and inhibitor of lipoprotein lipase. (2002) *J Lipid Res*. **11**, 1770-1772.

14. Mandard, S., Zandbergen, F., Tan, N. S., Escher, P., Patsouris, D., Koenig, W., Kleemann, R., Bakker, A., Veenman, F., Wahli, W., *et al.* The direct peroxisome proliferator-activated receptor target fasting-induced adipose factor (FIAF/PGAR/ANGPTL4) is present in blood plasma as a truncated protein that is increased by fenofibrate treatment. (2004) *J Biol Chem*. **33**, 34411-34420.

15. Xu, A., Lam, M. C., Chan, K. W., Wang, Y., Zhang, J., Hoo, R. L., Xu, J. Y., Chen, B., Chow, W. S., Tso, A. W., *et al.* Angiopoietin-like protein 4 decreases blood glucose and improves glucose tolerance but induces hyperlipidemia and hepatic steatosis in mice. (2005) *Proc Natl Acad Sci U S A*. **17**, 6086-6091.

16. Le Jan, S., Amy, C., Cazes, A., Monnot, C., Lamande, N., Favier, J., Philippe, J., Sibony, M., Gasc, J. M., Corvol, P., Germain, S. Angiopoietin-like 4 is a proangiogenic factor produced during ischemia and in conventional renal cell carcinoma. (2003) *Am J Pathol*. **5**, 1521-1528.

17. Lal, A., Peters, H., St Croix, B., Haroon, Z. A., Dewhirst, M. W., Strausberg, R. L., Kaanders. J. H., van der Kogel, A. J., Riggins, G. J. Transcriptional response to hypoxia in human tumors. (2001) *J Natl Cancer Inst*. **17**, 1337-1343.

18. Ito, Y., Oike, Y., Yasunaga, K., Hamada, K., Miyata, K., Matsumoto, S., Sugano, S., Tanihara, H., Masuho, Y., Suda, T. Inhibition of angiogenesis and vascular leakiness by angiopoietin-related protein 4. (2003) *Cancer Res*. **20**, 6651-6657.

19. Satkauskas, S., Bureau, M. F., Puc, M., Mahfoudi, A., Scherman, D., Miklavcic, D., Mir, L. M. Mechanisms of in vivo DNA electrotransfer: respective contributions of cell electropermeabilization and DNA electrophoresis. (2002) *Mol Ther*. **2**, 133-140.

20. Elie, N., Plancoulaine, B., Signolle, J. P., Herlin, P. A simple way of quantifying immunostained cell nuclei on the whole histologic section. (2003) *Cytometry A*. **1**, 37-45.

21. Ge, H., Yang, G., Yu, X., Pourbahrami, T., Li, C. Oligomerization state-dependent hyperlipidemic effect of angiopoietin-like protein 4. (2004) *J Lipid Res*. **11**, 2071-2079.

22. Koster, A., Chao, Y.B., Mosior, M., Ford, A., Gonzalez-DeWhitt, PA., Hale, JE., Li, D., Qiu, Y., Fraser, C.C., Yang, D.D., Heuer, J.G., Jaskunas, S.R., Eacho, P. Transgenic angiopoietin-like (angptl)4 overexpression and targeted disruption of angptl4 and angptl3: regulation of triglyceride metabolism.
Endocrinology. (2005) **146**:4943-4950.

23. Dhanabal, M., LaRochelle, W. J., Jeffers, M., Herrmann, J., Rastelli, L., McDonald, W. F., Chillakuru, R. A., Yang, M., Boldog. F. L., Padigaru, M., *et al.* Angioarrestin: an antiangiogenic protein with tumor-inhibiting properties. (2002) *Cancer Res.* **13**, 3834-3841.

24. Kubota, Y., Oike, Y., Satoh, S., Tabata, Y., Niikura, Y., Morisada, T., Akao, M., Urano, T., Ito, Y., Miyamoto, T., *et al*. Cooperative interaction of Angiopoietin-like proteins 1 and 2 in zebrafish vascular development. (2005) *Proc Natl Acad Sci U S A*. **102**, 13502-7.

25. Camenisch, G., Pisabarro, M. T ., Sherman, D., Kowalski, J., Nagel, M., Hass, P., Xie, M. H., Gurney, A., Bodary, S., Liang, X. H., *et al.* ANGPTL3 stimulates endothelial cell adhesion and migration via integrin alpha vbeta 3 and induces blood vessel formation in vivo. (2002) *J Biol Chem*. **19**, 17281-17290.

26. Thurston, G., Suri, C., Smith, K., McClain, J., Sato, T. N., Yancopoulos, G. D., McDonald, D. M. Leakage-resistant blood vessels in mice transgenically overexpressing angiopoietin-1. (1999) *Science*. **5449**, 2511-2514.

27. Burridge, K., Chrzanowska-Wodnicka, M. Focal adhesions, contractility, and signaling. (1996) *Annu Rev Cell Dev Biol*. **12**, 463-518.

28. Beavon, I. R. Regulation of E-cadherin: does hypoxia initiate the metastatic cascade? (1999) *Mol Pathol*. **4**, 179-188.

29. Ito, A., Katoh, F., Kataoka, T. R., Okada, M ., Tsubota, N., Asada, H., Yoshikawa, K., Maeda, S., Kitamura, Y., Yamasaki, H., *et al*. A role for heterologous gap junctions between melanoma and endothelial cells in metastasis. (2000) *J Clin Invest*. **9**, 1189-1197.

30. Hegerfeldt, Y., Tusch, M., Brocker, E. B, Friedl, P. Collective cell movement in primary melanoma explants: plasticity of cell-cell interaction, beta1-integrin function, and migration strategies. (2002) *Cancer Res*. **7**, 2125-2130.

31. Cardones, A.R., Murakami, T., Hwang, S. T. CXCR4 enhances adhesion of B16 tumor cells to endothelial cells in vitro and in vivo via beta(1) integrin. (2003) *Cancer Res*. **20**, 6751-7.

LEGENDS

Fig. 1: *In vivo angptl4* gene transfer by electrotransfer

Western blot analysis of ANGPTL4-mycHis protein detected by c-myc antibody. Sera from mice electrotransferred with control plasmid (week 2, lane 1) or with ANGPTL4 (week 2, lane 2 and week 6, lane 3), and from mice injected with 1μg of recombinant ANGPTL4 were analyzed (*A*). Assessment of plasma TG from mice injected, 30 min before, with control buffer or recombinant ANGPTL4 (1, 10 or 50µg), by enzymatic reaction (*B*).

Fig. 2: ANGPTL4 inhibits 3LL tumor cells intravasation, invasion of lymph nodes and lung metastases

Two weeks after muscle electroporation, C57/Bl6 mice were s.c. implanted with 3LL cells s.c. One, two, three, and four weeks after implantation, tumors, lymph nodes and lungs were removed and stained using HES and anti-CD34 immunohistochemistry. Invading tumor cells (emboli) were mainly observed in control mice (intratumor vessels, peritumor vessels, see arrows) (A). The number and the volume of metastatic lymph nodes (*B-left and right panel*) as well as the number of 3LL micrometastases in lungs (*C-left panel*) were quantified in sections from ANGPTL4 mice compared to control mice each week p.i.. Typical views of invaded lymph nodes (*B*-right panel; see the tumor area surrounded in black in control mouse *vs*. diffuse tumor cells shown by arrows in ANGPTL4 mice) and lung metastases (*C*-right panel).

Fig. 3: In B16F0 model, ANGPTL4 inhibits extravasation of tumor cells and macrometastases number

B16F0 cells were injected i.v. into C57/Bl6 mice two weeks after ANGPTL4 electroporation, and mice (12) were sacrificed either two or three weeks later. At week 2, tumor islets were observed in lungs by staining sections with HES (*A*, *top panel)* and anti-CD34 (*A*, *bottom panel*) allowing to discriminate micrometastases implanted in the lung parenchyma from intravascular emboli. Left panel, arrows indicate residual vascular walls associated with tumor cell extravasation in control lung. Right panel, arrows show intact vessels enclosing localized nodules (emboli) in lungs from ANGPTL4 mice (*A*). Quantification of micrometastases invaded the parenchyma of the lung (*B*) and localized emboli (*C*).

Typical views of lungs presenting macroscopic metastases at week 3 (*D, top panel*). For each mouse, quantification of total metastatic area (*E*) and mean surface area per macrometastasis (*F*) was performed using scanned images of HES-stained lung sections (*A, bottom panel*).

Fig. 4: Inhibition of histamine-induced vascular permeability by ANGPTL4

VP was evaluated by performing a Miles assay induced by histamine in *nude* mice electrotransferred with ANGPTL4 or control plasmid. Spectrophotometric analysis of vascular leakiness with Evans blue dye was performed. For each group, extravasation of dye after injection of histamine (1nM, 10nM) was compared with extravasation of dye after injection of PBS. Mean ng Evans blue per milligram of fresh tissue is represented ± SEM.

Figure 5: *In vitro* characterization of the overexpression of ANGPTl4 in tumor cells

Western blot analysis of ANGPTL4-mycHIS protein secreted by stably transfected B16F0 clones (B16F0/ANGPTL4-Low, -Medium or -High) compared to control cells (B16F0/Empty vector as negative control and CHO/ANGPTL4 as positive control (15) and detected by c-myc antibody (*A*).

- Alteration of tumor cell adhesion, motility and invasiveness and by ANGPTL4

"Adhesion assay": 5.10^4 stained B16F0 cells expressing ANGPTL4 or control cells were plated on BSA, fibronectin, laminin or vitronectin for 1h and fluorescence was measured (*B*). "Boyden chamber assay": 1.10^5 stained cells expressing ANGPTL4 or control cells were seeded in transwells with polycarbonate membrane plates. Migration on a fibronectin coating or invasion through a Matrigel barrier was induced using conditionned medium from 3T3 cells. After six hours, migration or invasion was assessed by measuring fluorescence *(C)*.

- ANGPTL4 modifies cytoskeleton organization

Cytoskeleton organization of B16F0 ANGPTL4 cells or control cells was evaluated by fluorescence detection of polymerized actin fibers (red) and vinculin (green) on fibronectin or BSA coating supports (*E*). Quantification was performed by determining the percentage of cells showing an organized cytoskeleton i.e. polymerized actin stress fibers (red) and vinculin focal adhesion contacts (green) in control and ANGPTL4 cells on fibronectin or BSA (*F*).

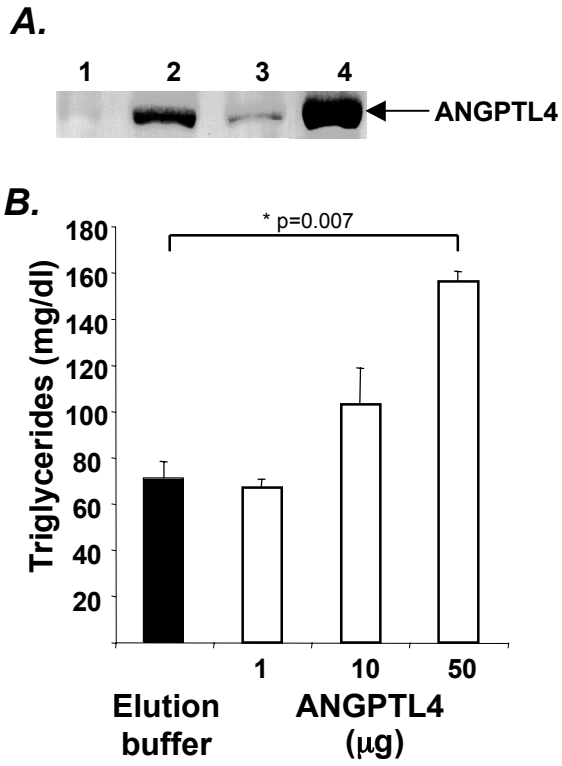

FIG. 1

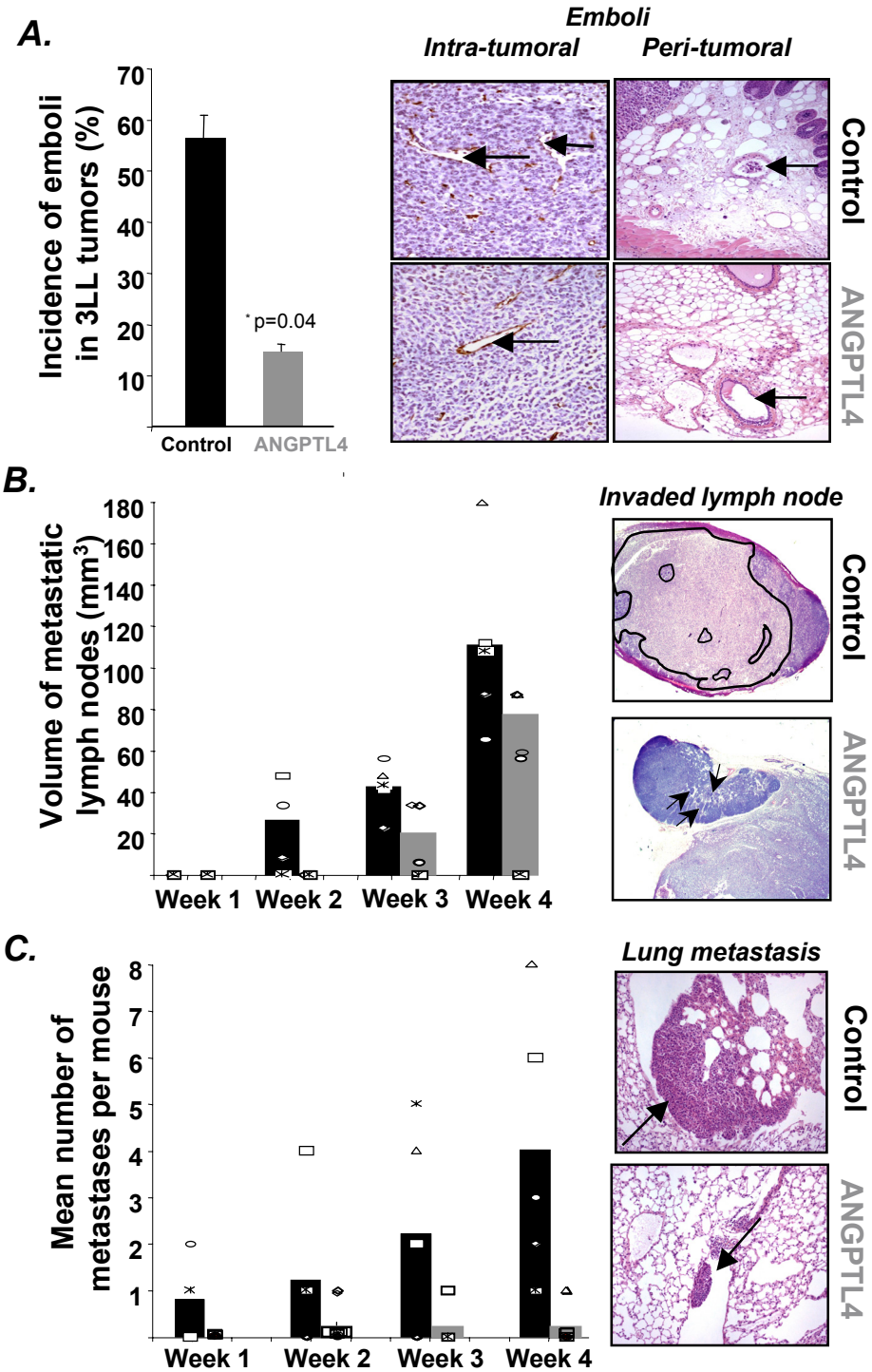

FIG. 2

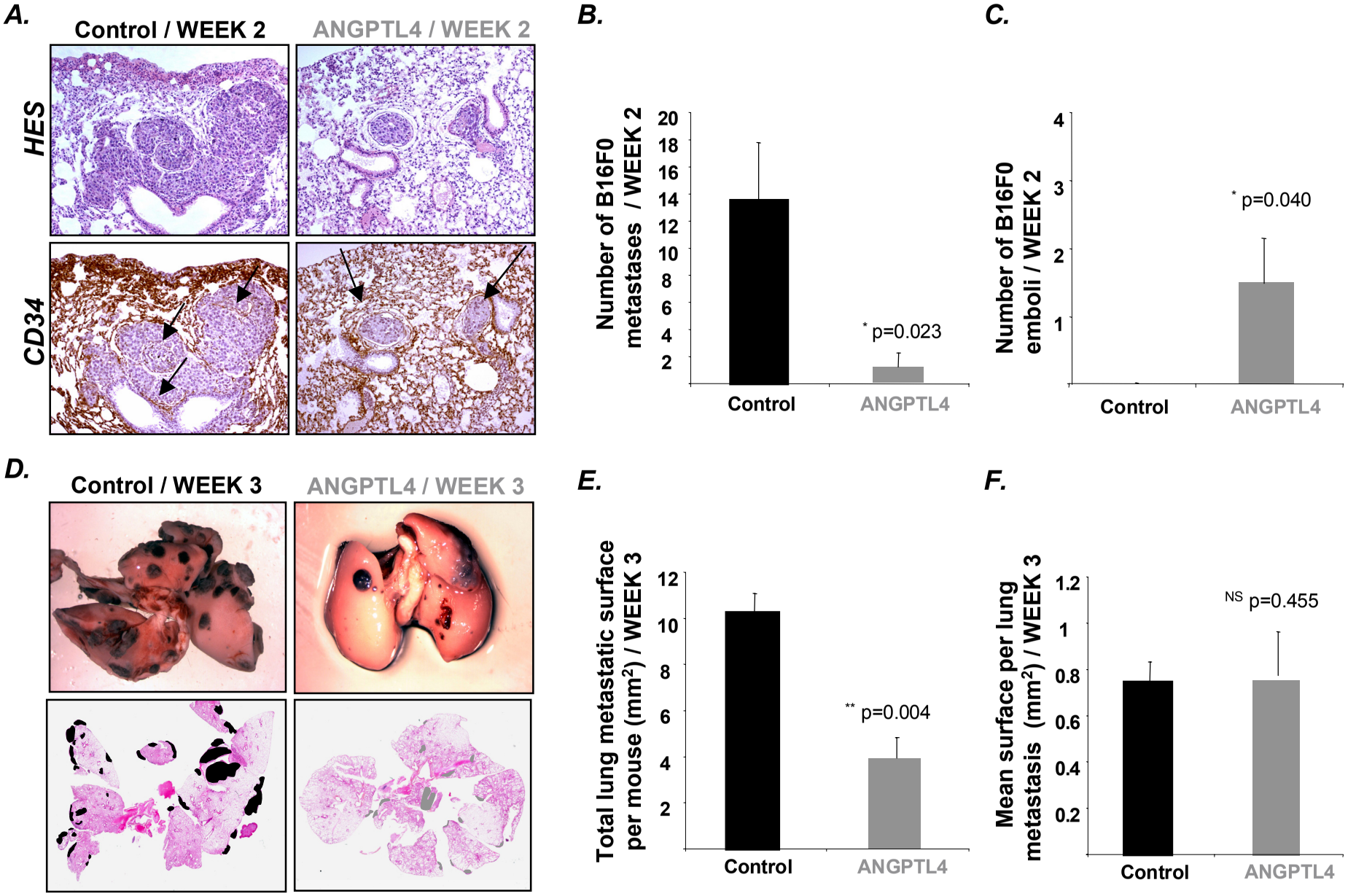

FIG. 3

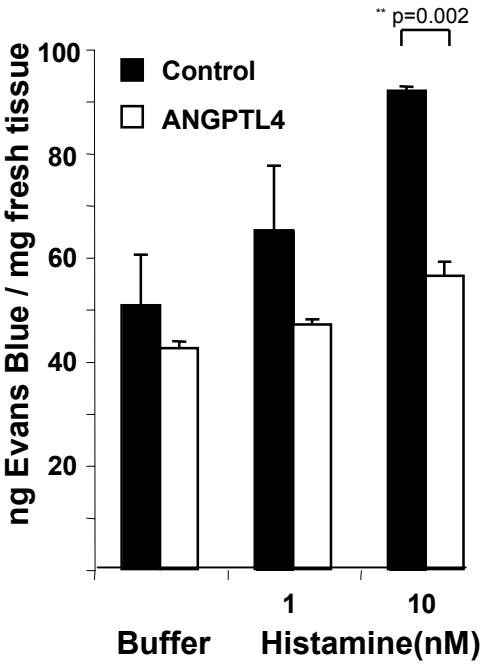

FIG. 4

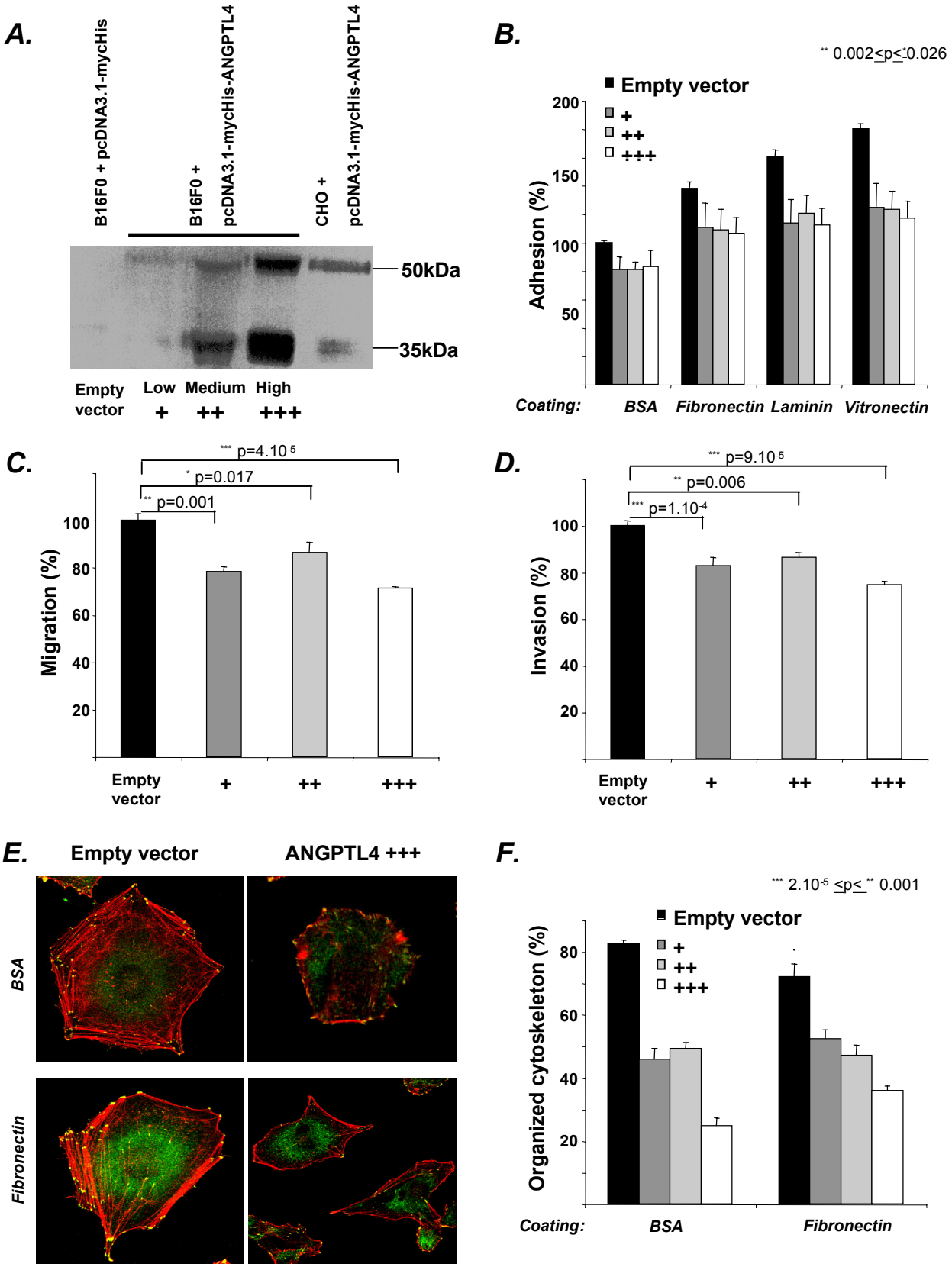

Fig. 5